

Resonance-fluorescence and absorption spectra of a two-level atom driven by a strong bichromatic field

Z. Ficek

Department of Physics, The University of Queensland, Brisbane, Queensland 4072, Australia

H. S. Freedhoff

Department of Physics and Astronomy, York University, Toronto, Canada M3J 1P3

(Received 13 July 1992; revised manuscript received 20 April 1993)

We examine the radiative properties of a two-level atom driven by a strong bichromatic field with frequencies $\omega_1 = \omega_0 - \delta_1$ and $\omega_2 = \omega_0 + \delta_2$, which can be asymmetrically placed about the atomic transition frequency ω_0 and can have different Rabi frequencies Ω_1 and Ω_2 . Applying the optical Bloch equations for the bichromatic excitation, we derive an infinite set of equations of motion for the time evolution of the atomic variables. The equations are solved numerically by matrix inversion and Laplace transforms. Using the quantum regression theorem, we then solve for the steady-state total fluorescence intensity, and the resonance-fluorescence and absorption spectra. The spectra are found to depend on the frequency difference $2\delta = \delta_1 + \delta_2$, the average detuning $\Delta = \omega_0 - \frac{1}{2}(\omega_1 + \omega_2)$, and the Rabi frequencies of the driving fields. For $\Omega_1 = \Omega_2 = \Omega$, the total fluorescent intensity displays a series of maxima for $\Delta = \pm n\delta \mp \Omega^2/4\delta$, where the n are the odd integers. The intensity-dependent shift from the resonances $n\delta$ is explained as an analog of the generalized Bloch-Siegert shift. The resonance-fluorescence spectrum for $\Delta \neq 0$ appears to contain more peaks than that for $\Delta = 0$. This is due to the splitting of the central peak and the even sidebands into doublets. The absorption spectrum of a weak-probe beam for $\Delta = 0$ and equal Rabi frequencies consists of a symmetric series of dispersionlike sidebands separated from ω_0 by integer multiples of δ , together with a central absorption peak at ω_0 , whose amplitude oscillates with Ω . For $\Delta \neq 0$ and/or $\Omega_1 \neq \Omega_2$, the odd sidebands remain dispersionlike, while the central peak and the even sidebands split into absorption-emission doublets. A simple physical interpretation of the spectral features is given in terms of the dressed-atom model.

PACS number(s): 32.80.-t, 42.50.Hz

I. INTRODUCTION

Resonance fluorescence, or the resonant interaction of electromagnetic radiation with an atomic system, has received considerable attention in recent years. When an excited atom decays into the vacuum, the emitted radiation has an isotropic distribution in space and its spectrum is a Lorentzian function of frequency with a linewidth proportional to the Einstein spontaneous-decay rate. The fluorescence spectrum can be altered in a fundamental way, however, by driving the atom with a sufficiently strong resonant field. In fact, a three-peaked fluorescence spectrum has been both predicted [1–4] and observed [5] when the atom is driven by a strong monochromatic resonant field. The sidebands, which are $\frac{1}{3}$ as high as the central peak, are shifted from that peak by an amount equal to the Rabi frequency Ω of the driving field, and are wider than it by a factor of 1.5. For a strong, nonresonant driving field the spectrum retains its three-peaked structure, but is asymmetric in the transient regime [6]. This asymmetry can persist into the steady state if the driving field has a finite bandwidth [7]. The effect on a weak probe beam of a strongly driven atom has also been studied theoretically [8–10], and experimentally observed by Wu *et al.* [11]. Here again a three-peaked spectrum is obtained, reminiscent of the two-level-system resonance-fluorescence spectrum. However,

when the driving-field frequency is equal to the atomic frequency, the central component disappears and the weak-probe absorption profile exhibits dispersionlike features at $\pm\Omega$. For an off-resonant driving field, the absorption profile (spectrum) consists of one absorption and one emission component at $\pm\Omega$, indicating that, in one sideband, stimulated emission outweighs absorption, so that the probe beam is amplified at the expense of the driving field. Many features of the fluorescence and absorption spectra can be conveniently explained in terms of a “dressed-atom” description of the atom-field interaction [4,12]. In the dressed-atom approach, eigenstates of the atom-plus-driving-field system serve as the basis states of the system. The components of the fluorescence and absorption spectra are viewed as arising from transitions between these dressed states.

Recently, an experiment was reported [13] and a theory was developed [14–17] for the fluorescence spectrum of a two-level atom driven by a strong bichromatic field. The spectrum differs in many important respects from the characteristic three-peaked spectrum that is observed for strong monochromatic excitation. Under bichromatic excitation, the spectrum consists of a series of peaks with a constant spacing δ , where 2δ is the frequency difference between the two driving fields. The peak separations are independent of the Rabi frequencies Ω of the driving fields, but the number of peaks in the spec-

trum increases with increasing Ω , and their amplitudes oscillate. The peaks separated from ω_0 by even multiples of δ (even sidebands) have different linewidths than those separated from ω_0 by odd multiples of δ (odd sidebands). These results have a simple interpretation in terms of the dressed states of the system and the possible transitions among them [15]. In the case of bichromatic excitation, the energy spectrum of the uncoupled atom-field product states consists of manifolds of states separated by integer multiples of δ . Inclusion of the atom-field coupling leads to the dressed states, which are superpositions of the uncoupled product states. For any product state within a manifold, the coupling to the states above and below it is symmetric. Due to this symmetry, the energy separation between neighboring dressed states is also δ . The multipeak spectrum can be interpreted as a result of transitions between the dressed-state sublevels. Fluorescence spectra that display some of the same features as those described for bichromatic excitation have also been predicted for a two-level atom in an amplitude-modulated field [18–24], and for a two-level atom in a continuous pulse-train field [25].

Most previous studies involving bichromatic excitation have dealt with the case of equal Rabi frequencies and ω_0 in resonance with the average frequency of the driving fields, i.e., the detuning Δ between ω_0 and $(\omega_1 + \omega_2)/2$ was zero. In the experimental study [13] the fluorescence spectrum shows marked asymmetry and apparently contains more peaks, when $\Delta \neq 0$. No explanation has been offered so far for the appearance of the large number of peaks. Moreover, recent studies of the generalized Bloch-Siegert shifts [21] and Doppleron cooling [26] in a fully modulated field show an important role of the detuning Δ at values corresponding to subharmonic and Doppleron resonances.

It is our purpose in this paper to study resonance fluorescence from a two-level atom driven by an off-resonance bichromatic field and the probe-beam absorption spectrum under resonant as well as nonresonant bichromatic excitation. We work with the optical Bloch equations. We find that the steady-state intensity spectrum exhibits maxima at $\Delta = \pm n\delta \mp \Omega^2/4\delta$, where the n are the odd integers. The intensity-dependent term in these frequencies is the analog of the generalized Bloch-Siegert shift [21]. We also find that for $\Delta \neq 0$ the fluorescence spectrum contains more peaks due to splitting of the central peak and the even sidebands into doublets. The main result of this work is the probe-beam absorption spectrum of a two-level atom driven by a strong bichromatic field. It is shown that the probe absorption spectrum depends on the frequency difference 2δ , detuning Δ , and the Rabi frequencies Ω_1 and Ω_2 of the two driving fields, and differs from that for monochromatic excitation. When $\Delta = 0$ and $\Omega_1 = \Omega_2 = \Omega$, the spectrum shows a symmetric series of dispersionlike sidebands separated by the constant spacing δ , surrounding a central absorption peak whose amplitude oscillates with Ω , reflecting an oscillation in the average atomic inversion [19–23,27]. For $\Delta \neq 0$ and $\Omega_1 = \Omega_2$ the spectrum contains a series of dispersionlike odd sidebands, together with absorption-emission doublets centered at ω_0 and at the

even sideband frequencies. Similar spectral features are found for $\Delta = 0$ and unequal Rabi frequencies.

This paper is organized as follows. The optical Bloch equations for a two-level atom in a bichromatic field are developed in Sec. II. The steady-state solutions of these equations and the intensity (power) spectrum are discussed in Sec. III. In Sec. IV we study the effect of Δ on the fluorescence spectrum. The absorption spectrum of a weak-probe beam is calculated in Sec. V. Finally, the dressed-atom picture of the spectral features is presented in Sec. VI.

II. OPTICAL BLOCH EQUATIONS

Consider a two-level atom with excited and ground states denoted, respectively, by $|e\rangle$ and $|g\rangle$ and separated by frequency ω_0 . The atom may be described as a spin- $\frac{1}{2}$ system, characterized by the standard spin angular momentum operators $S^\pm(t)$ and $S^z(t)$ satisfying the commutation relations

$$\begin{aligned} [S^+(t), S^-(t)] &= 2S^z(t), \\ [S^z(t), S^\pm(t)] &= \pm S^\pm(t). \end{aligned} \quad (2.1)$$

The bichromatic driving field is

$$\mathbf{E}(t) = [\mathbf{E}_1 \exp(-i\omega_1 t) + \mathbf{E}_2 \exp(-i\omega_2 t)] + \text{c.c.}, \quad (2.2)$$

where $\omega_1 = \omega_0 - \delta_1$ and $\omega_2 = \omega_0 + \delta_2$ are the frequencies of the bichromatic field, and $\mathbf{E}_{1,2}$ are its amplitudes. We assume that the frequencies ω_1 and ω_2 are not symmetrically placed about ω_0 (see Fig. 1), and are separated by $2\delta = \delta_1 + \delta_2$. Since $\delta_1 \neq \delta_2$ there is a net detuning $\Delta = \omega_0 - \omega_s$ between the atomic frequency and the average frequency $\omega_s = (\omega_1 + \omega_2)/2$ of the driving fields. Denoting the Rabi frequencies of the driving fields by

$$\Omega_1 = 2\boldsymbol{\mu} \cdot \mathbf{E}_1 / \hbar, \quad \Omega_2 = 2\boldsymbol{\mu} \cdot \mathbf{E}_2 / \hbar, \quad (2.3)$$

where $\boldsymbol{\mu}$ is the atomic transition electric dipole moment, we write the optical Bloch equations, in a frame rotating with the average frequency ω_s and in the rotating-wave approximation, in the form

$$\frac{d}{dt} \mathbf{X} = \underline{A} \mathbf{X} + \mathbf{v}, \quad (2.4)$$

where \underline{A} is the 3×3 matrix

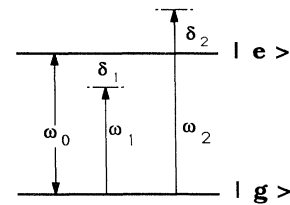


FIG. 1. Two-level atom driven by two coherent fields of frequencies $\omega_1 = \omega_0 - \delta_1$ and $\omega_2 = \omega_0 + \delta_2$.

$$\underline{A} = \begin{pmatrix} -(\frac{1}{2}\Gamma + i\Delta) & 0 & \Omega(e^{i\delta t} + \alpha e^{-i\delta t}) \\ 0 & -(\frac{1}{2}\Gamma - i\Delta) & \Omega(e^{-i\delta t} + \alpha e^{i\delta t}) \\ -\frac{1}{2}\Omega(e^{-i\delta t} + \alpha e^{i\delta t}) & -\frac{1}{2}\Omega(e^{i\delta t} + \alpha e^{-i\delta t}) & -\Gamma \end{pmatrix} \quad (2.5)$$

and \mathbf{X} is a column vector with complex components

$$\begin{aligned} X_1(t) &= \langle S^-(t) \rangle e^{i(\omega_s t + \Psi_L)}, \\ X_2(t) &= \langle S^+(t) \rangle e^{-i(\omega_s t + \Psi_L)}, \\ X_3(t) &= \langle S^z(t) \rangle. \end{aligned} \quad (2.6)$$

The components of the column vector \mathbf{v} are given by

$$v_i = -\frac{1}{2}\Gamma\delta_{3,i}. \quad (2.7)$$

Here $\Omega = \Omega_1$, $\alpha = \Omega_2/\Omega_1$, Ψ_L is a phase angle, assumed to be equal for the two driving fields, and Γ is the Einstein A coefficient for spontaneous emission.

Different numerical and analytical methods [14–17] have been used to solve Eq. (2.4). Here we propose a method, similar to a Floquet technique, which transforms the system of Eqs. (2.4) with time-dependent coefficients into a system consisting of an infinite number of equations with time-independent coefficients. This latter system is solved numerically by matrix inversion. To do this we decompose the components $X_i(t)$ into slowly varying amplitudes that oscillate at the modulation frequency δ and its harmonics. This decomposition is given by the relation

$$X_i(t) = \sum_{l=-\infty}^{+\infty} X_i^{(l)}(t) e^{il\delta t}. \quad (2.8)$$

On substituting (2.8) into (2.4), we find the slowly varying amplitudes $X_i^{(l)}(t)$ to obey the system of equations

$$\begin{aligned} \frac{d}{dt} X_1^{(l)}(t) &= -(\frac{1}{2}\Gamma + i\Delta + il\delta) X_1^{(l)}(t) \\ &\quad + \Omega[\alpha X_3^{(l+1)}(t) + X_3^{(l-1)}(t)], \\ \frac{d}{dt} X_2^{(l)}(t) &= -(\frac{1}{2}\Gamma - i\Delta + il\delta) X_2^{(l)}(t) \\ &\quad + \Omega[X_3^{(l+1)}(t) + \alpha X_3^{(l-1)}(t)], \\ \frac{d}{dt} X_3^{(l)}(t) &= -\frac{1}{2}\Gamma\delta_{l,0} - (\Gamma + il\delta) X_3^{(l)}(t) \\ &\quad - \frac{1}{2}\Omega\alpha[X_1^{(l-1)}(t) + X_2^{(l+1)}(t)] \\ &\quad - \frac{1}{2}\Omega[X_1^{(l+1)}(t) + X_2^{(l-1)}(t)]. \end{aligned} \quad (2.9)$$

We solve Eq. (2.9) by Laplace transform methods, which lead to the following system of algebraic equations for the transforms $X_i^{(l)}(z)$:

$$\begin{aligned} (z_l + \frac{1}{2}\Gamma + i\Delta) X_1^{(l)}(z) &= X_1^{(l)}(0) + \Omega[\alpha X_3^{(l+1)}(z) + X_3^{(l-1)}(z)], \\ (z_l + \frac{1}{2}\Gamma - i\Delta) X_2^{(l)}(z) &= X_2^{(l)}(0) + \Omega[X_3^{(l+1)}(z) + \alpha X_3^{(l-1)}(z)], \\ (z_l + \Gamma) X_3^{(l)}(z) &= X_3^{(l)}(0) - \frac{\Gamma}{2z} \delta_{l,0} \\ &\quad - \frac{1}{2}\Omega[X_1^{(l+1)}(z) + X_2^{(l-1)}(z)] \\ &\quad - \frac{1}{2}\Omega\alpha[X_1^{(l-1)}(z) + X_2^{(l+1)}(z)], \end{aligned} \quad (2.10)$$

where $z_l = z + il\delta$, with z the complex Laplace transform variable, and $X_i^{(l)}(0)$ the initial values of the components $X_i^{(l)}(t)$.

On eliminating $X_1^{(l)}(z)$ and $X_2^{(l)}(z)$, we transform Eq. (2.10) into the system of equations

$$a_l X_3^{(l)}(z) + b_l X_3^{(l-2)}(z) + d_l X_3^{(l+2)}(z) = g_l, \quad (2.11)$$

where

$$\begin{aligned} a_l &= (z_l + \Gamma) + \frac{1}{2}\Omega^2 \left[\frac{\alpha^2}{P_{l-1}} + \frac{1}{Q_{l-1}} + \frac{1}{P_{l+1}} + \frac{\alpha^2}{Q_{l+1}} \right], \\ b_l &= d_{l-2} = \frac{1}{2}\Omega^2 \alpha \left[\frac{1}{P_{l-1}} + \frac{1}{Q_{l-1}} \right], \\ g_l &= X_3^{(l)}(0) - \frac{\Gamma}{2z} \delta_{l,0} - \frac{1}{2}\Omega \left[\frac{\alpha X_1^{(l-1)}(0)}{P_{l-1}} + \frac{X_1^{(l+1)}(0)}{P_{l+1}} \right] \\ &\quad - \frac{1}{2}\Omega \left[\frac{X_2^{(l-1)}(0)}{Q_{l-1}} + \frac{\alpha X_2^{(l+1)}(0)}{Q_{l+1}} \right], \end{aligned} \quad (2.12)$$

and

$$\begin{aligned} P_l &= (z + il\delta + \frac{1}{2}\Gamma + i\Delta), \\ Q_l &= (z + il\delta + \frac{1}{2}\Gamma - i\Delta). \end{aligned} \quad (2.13)$$

We construct an infinite-dimensional column vector \mathbf{Y} by putting together the amplitudes $X_3^{(l)}(z)$ in the order

$$\mathbf{Y} = \begin{pmatrix} \vdots \\ X_3^{(1)}(z) \\ X_3^{(0)}(z) \\ X_3^{(-1)}(z) \\ \vdots \end{pmatrix}. \quad (2.14)$$

Equation (2.11) can then be written as

$$\underline{K}\mathbf{Y} = \mathbf{P}, \quad (2.15)$$

Figure 2 shows the steady-state fluorescence intensity as a function of the detuning Δ for a bichromatic excitation with $\alpha=1$, $\delta=5\Gamma$, and different values of Ω . For a weak driving field the intensity spectrum consists of two distinct peaks centered at the frequencies $\omega_s = \omega_0 \pm \delta$. As the driving-field intensity increases these two peaks shift towards smaller Δ and simultaneously become power broadened; in addition, there appear new peaks near $\Delta = \pm 15\Gamma$. Increasing the driving-field intensity still more, these peaks also shift towards smaller Δ , and there appear an additional two peaks at larger Δ . These graphs show that the intensity spectrum consists of many peaks located near $\Delta = \pm n\delta$, where n is an odd integer, and that these peaks move towards smaller Δ as Ω increases. To explain this, we will approximately solve the set of equations (2.11) in terms of continued fractions. With the parameters (3.7), for $l=0$ and in the lowest approximation, we ignore the coupling of $X_3^{(0)}$ to $X_3^{(2)}$ and $X_3^{(-2)}$ and find from Eq. (2.11) that

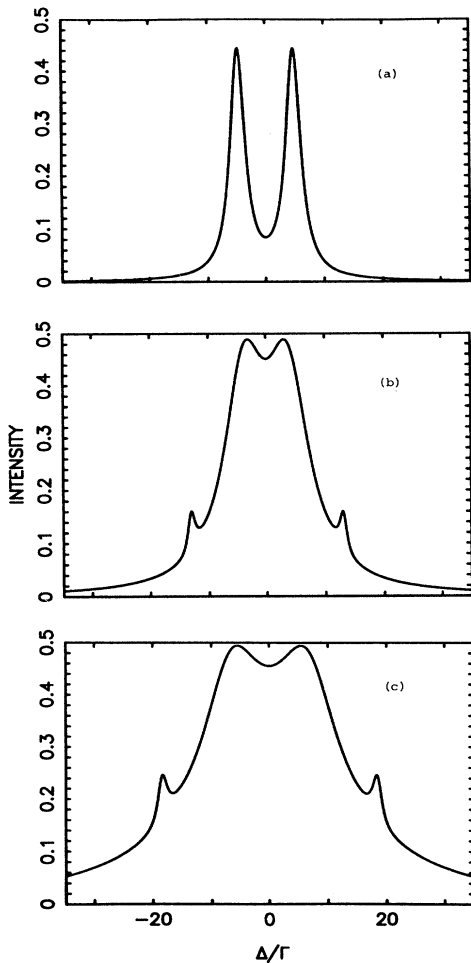


FIG. 2. The steady-state intensity spectrum as a function of the detuning Δ for bichromatic excitation with $\alpha=1$, $\delta=5\Gamma$, and different Rabi frequencies: (a) $\Omega=2\Gamma$, (b) $\Omega=5\Gamma$, (c) $\Omega=12\Gamma$.

$$X_3^{(0)} = -\frac{1}{2}\Gamma \left\{ \Gamma + \frac{1}{2}\Omega^2 \left[\frac{\Gamma}{\frac{1}{4}\Gamma^2 + (\Delta - \delta)^2} + \frac{\Gamma}{\frac{1}{4}\Gamma^2 + (\Delta + \delta)^2} \right] \right\}^{-1}. \quad (3.9)$$

Near the resonance $\Delta \approx \delta$ only the first Lorentzian contributes to the spectrum, and the intensity I_{SS} is

$$I_{SS} = \frac{1}{4} \frac{\Gamma\Omega^2}{[\frac{1}{4}\Gamma^2 + \frac{1}{2}\Omega^2 + (\Delta - \delta)^2]}. \quad (3.10)$$

Similarly, near the resonance $\Delta \approx -\delta$ only the second Lorentzian in (3.9) contributes, and we find

$$I_{SS} = \frac{1}{4}\Gamma \frac{\Omega^2}{[\frac{1}{4}\Gamma^2 + \frac{1}{2}\Omega^2 + (\Delta + \delta)^2]}. \quad (3.11)$$

Thus, in the lowest approximation, which corresponds to a weak driving field, the intensity spectrum consists of two peaks located at $\Delta = \pm\delta$, with power broadened widths.

In the next approximation we include the coupling of $X_3^{(0)}$ to $X_3^{(-2)}$ and $X_3^{(2)}$, and we find

$$X_3^{(0)} = -\frac{\Gamma}{2} \left[a_0 - \frac{b_0^2}{a_{-2}} - \frac{b_2^2}{a_2} \right]^{-1}. \quad (3.12)$$

Near the resonances $\Delta \approx \pm\delta$ ($\delta \gg \Gamma$), this reduces to

$$X_3^{(0)} = -\frac{1}{2} \left\{ 1 - \frac{\frac{1}{2}\Omega^2}{[\frac{1}{4}\Gamma^2 + \frac{1}{2}\Omega^2 + (\Delta \mp \delta \pm \Omega^2/4\delta)^2]} \right\}. \quad (3.13)$$

Thus the spectrum contains two Lorentzians with frequencies shifted from $\pm\delta$ by the amount $\Omega^2/4\delta$. From expression (3.12), we see that it also contains additional resonances at $\Delta \approx \pm 3\delta$, because the parameters a_2 and a_{-2} contain terms $(\Delta \pm 3\delta)$. It is not difficult to show from Eq. (2.11) that in successively higher approximations $X_3^{(0)}$ contains resonant terms at $(\Delta \pm n\delta)$, where $n=1, 3, 5, \dots$. It may be added here that the power-dependent shifts of the resonances at $\Delta = \pm n\delta$ are the analog of the optical Bloch-Siegert shift which occurs in the case of a monochromatic field interacting with a two-level atom without the rotating-wave approximation [31,32]. This level shift, named the generalized Bloch-Siegert shift, has also been studied for a fully amplitude-modulated field interacting with a two-level atom [21,33-36]. A fully amplitude-modulated field is the complete equivalent of a bichromatic field.

IV. RESONANCE-FLUORESCENCE SPECTRUM

The steady-state resonance-fluorescence spectrum is given by the Fourier transform of the two-time correlation function of the scattered electric field

$$S(\omega) = \text{Re} \int_0^\infty d\tau e^{i\omega\tau} \lim_{t \rightarrow \infty} \langle \mathbf{E}^{(-)}(\mathbf{r}, t) \cdot \mathbf{E}^{(+)}(\mathbf{r}, t + \tau) \rangle. \quad (4.1)$$

Since the electric field operator $\mathbf{E}^{(+)}(\mathbf{r}, t)$ far from the atomic system is simply proportional to the atomic operator $S^-(t-r/c)$, we have from Eqs. (4.1) and (3.2)

$$S(\omega) = \Gamma u(\hat{\mathbf{r}}) \text{Re} \int_0^\infty d\tau e^{i\omega\tau} G(\tau), \quad (4.2)$$

where

$$G(\tau) = \lim_{t \rightarrow \infty} \langle S^+(t) S^-(t+\tau) \rangle, \quad (4.3)$$

and we have replaced the retarded time $t-r/c$ by t as the correlation function is calculated in the steady state.

Introducing the Laplace transform, we express the fluorescence spectrum in the form

$$S(\omega) = \Gamma u(\hat{\mathbf{r}}) \text{Re} G(z) \Big|_{z=-i\nu}, \quad (4.4)$$

where $\nu = (\omega - \omega_s)/\Gamma$, and $G(z)$ denotes the Laplace transform of the atomic correlation function $G(\tau)$. In order to compute the fluorescence spectrum we have to compute the Laplace transform of the atomic correlation function $G(\tau)$. From the quantum regression theorem [37], it is well known that for $\tau > 0$ the two-time average $\langle S^+(t) S^-(t+\tau) \rangle$ satisfies the same equation of motion as the one-time average $\langle S^-(\tau) \rangle$. It is not difficult to show that the optical Bloch equations (2.4) for the two-time averages lead to equations of the same form as (2.11), but with coefficients g_l given by

$$g_l = X_3^{(l)}(t) - \frac{\Gamma}{2z} \langle S^+(t) \rangle \delta_{l,0} - \frac{1}{2} \Omega \left[\frac{\alpha X_1^{(l-1)}(t)}{P_{l-1}} + \frac{X_1^{(l+1)}(t)}{P_{l+1}} \right], \quad (4.5)$$

where $X_i^{(l)}(t)$ are the initial values of the correlations, and are given in terms of the single-time expectation values by

$$\begin{aligned} X_3^{(l)}(t) &= -\frac{1}{2} \langle S^+(t) \rangle e^{-il\delta t}, \\ X_1^{(l)}(t) &= \langle S^z(t) + \frac{1}{2} \rangle e^{-il\delta t}. \end{aligned} \quad (4.6)$$

Since the steady state only the zero-order component of $X_1(t+\tau) = \langle S^+(t) S^-(t+\tau) \rangle$ contributes to the spectrum, we can easily compute the spectrum by having recourse to the definition (4.4) and Eqs. (2.11)–(2.13) and (4.5). The Laplace transform $X_1^{(0)}(z)$ of the component $X_1^{(0)}(t+\tau)$ has a contribution from the pole at $z=0$ [see Eq. (4.5)]. This reflects the presence of the coherent scattering peaks in the (complete) spectrum $S(\omega)$. The incoherent spectrum $S_{\text{in}}(\omega)$ can be calculated by subtracting out the coherent peaks in the usual way:

$$S_{\text{in}}(\omega) = \Gamma u(\hat{\mathbf{r}}) \text{Re} U^{(0)}(-i\nu), \quad (4.7)$$

where $U^{(0)}(z)$ is the zero-order component of

$$U(z) = X_1(z) - \frac{1}{z} \lim_{z \rightarrow 0^+} z X_1(z). \quad (4.8)$$

To obtain the amplitude $X_1^{(0)}(z)$ we require $X_3^{(-1)}(z)$ and $X_3^{(1)}(z)$. We find $X_3^{(l)}(z)$ by numerical solution of Eq. (2.15) with coefficients a_l , b_l , and d_l given in Eq. (2.12), and g_l given in Eq. (4.5).

The incoherent fluorescence spectrum (4.7), which in-

corporates (4.8), provides the explicit expression for the fluorescence spectrum of a two-level atom in a bichromatic field. In Fig. 3 the spectrum is shown for $\alpha=1$, $\delta=5\Gamma$, $\Omega=8\Gamma$, and different values of Δ . For $\Delta=0$ the spectrum shows the well-known structure, experimentally observed by Mossberg and co-workers [13], consisting of a central peak at $\nu=0$, and a series of peaks with a constant spacing δ . As the detuning Δ comes into play, the central peak and the peaks separated from ω_s by even multiples of δ (even sidebands) start to split into doublets. For larger Δ ($\Delta \gg \Gamma$), this splitting is larger than the widths of the lines and the components of the doublets are very well resolved. As a result, the spectrum consists of more peaks than that for $\Delta=0$. The amplitudes of the peaks at positive ν are substantially larger than those at negative ν . It may be noticed that the positions of the peaks separated from ω_s by odd multiples of δ (odd sidebands) are independent of Δ . Agarwal *et al.* [17] have noted that the fluorescence spectrum shows marked asymmetry and apparently contains more peaks, when $\Delta \neq 0$. Beyond this comment, previous authors have said nothing about the appearance of the larger number of peaks. We explain these features in terms of

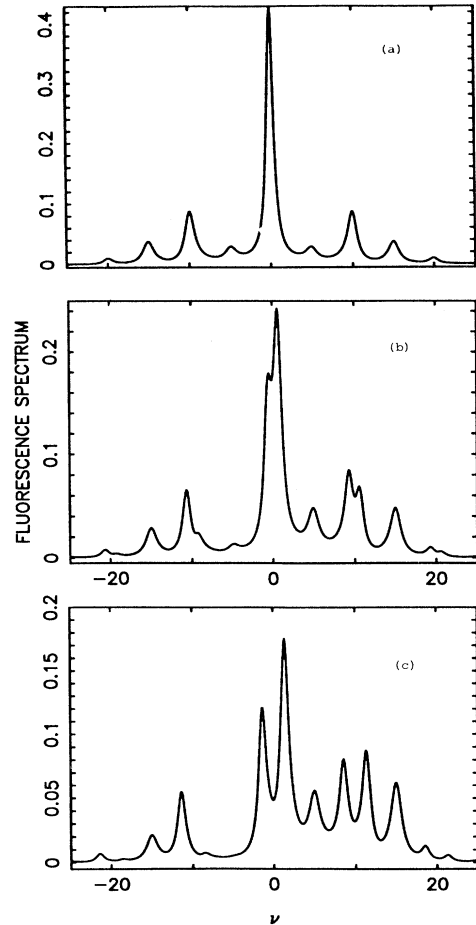


FIG. 3. The fluorescence spectrum as a function of $\nu = (\omega - \omega_s)/\Gamma$ for $\alpha=1$, $\delta=5\Gamma$, $\Omega=8\Gamma$, and detunings (a) $\Delta=0$, (b) $\Delta=2\Gamma$, (c) $\Delta=4\Gamma$.

the dressed-atom model of the system, which will be discussed in Sec. VI.

It is interesting to note that the incoherent fluorescence spectrum also shows the larger number of peaks when $\Delta=0$ and $\alpha \neq 1$ (unequal Rabi frequencies). This is shown in Fig. 4, where we plot the spectrum for $\Delta=0$, $\delta=5\Gamma$, $\Omega=8\Gamma$, and different values of α . For $\alpha \neq 1$, as for $\Delta \neq 0$, the central peak and the even sidebands split into doublets, whereas the frequencies of the odd sidebands are independent of α . These features are also explained in Sec. VI.

V. PROBE-BEAM ABSORPTION SPECTRUM

Consider a two-level atom driven by a bichromatic field and simultaneously illuminated by a tunable probe field of frequency ω_p and amplitude \mathbf{E}_p , which is assumed to be sufficiently weak that it does not appreciably perturb the atomic evolution. According to the linear-response theory [8,38], the steady-state absorption spectrum of the probe beam is given in terms of the Fourier transform of the average value of the two-time commuta-

tor of the atomic operators as

$$W(\omega_p) = W_0 \text{Re} \int_0^\infty d\tau e^{i\omega_p \tau} D(\tau), \quad (5.1)$$

where

$$W_0 = 2\omega_p \Gamma u(\hat{\mathbf{r}}) |\boldsymbol{\mu} \cdot \mathbf{E}_p|^2 / \hbar, \quad (5.2)$$

$$D(\tau) = \lim_{t \rightarrow \infty} \langle [S^-(t+\tau), S^+(t)] \rangle, \quad (5.3)$$

and the commutator is calculated in the absence of the probe beam, but with the driving field present.

Note that the absorption spectrum calculated here differs from that discussed by Nayak and Agarwal [23,39] and others [22,40]. They discussed the absorption of a probe beam of arbitrary intensity by a two-level atom pumped by a strong monochromatic field. In our model the atom is pumped by a bichromatic field and probed by a weak beam.

Using Laplace transforms, we rewrite the absorption spectrum (5.1) in the form

$$W(\omega_p) = W_0 \text{Re} D(z) |_{z=-i\eta}, \quad (5.4)$$

where $\eta = (\omega_p - \omega_s) / \Gamma$, and $D(z)$ is the Laplace transform of the commutator $D(\tau)$. From the quantum regression theorem, we know that the commutator $D(\tau)$ satisfies the same equation of motion as $\langle S^-(\tau) \rangle$. For the two-time commutator $D(\tau)$ the optical Bloch equations (2.4) lead to the same equation as (2.11), but with coefficients g_l given by

$$g_l = X_3^{(l)}(t) - \frac{1}{2} \Omega \left[\frac{\alpha X_1^{(l-1)}(t)}{P_{l-1}} + \frac{X_1^{(l+1)}(t)}{P_{l+1}} \right], \quad (5.5)$$

where

$$X_3^{(l)}(t) = \langle S^+(t) \rangle e^{-il\delta t}, \quad (5.6)$$

$$X_1^{(l)}(t) = -2 \langle S^z(t) \rangle e^{-il\delta t}.$$

The spectrum can be plotted using Eq. (5.4), which in terms of the components $X_i^{(l)}$ takes the following form:

$$W(\omega_p) = W_0 \text{Re} X_1^{(0)}(z) |_{z=-i\eta}. \quad (5.7)$$

To obtain the amplitude $X_1^{(0)}(z)$ we require $X_3^{(\pm 1)}(z)$, which we find by numerical solution of the system of equations (2.15) with coefficients a_l , b_l , and d_l given in Eq. (2.12) and g_l given in Eq. (5.5).

We first consider the absorption spectrum for a resonant bichromatic field ($\Delta=0$) and equal Rabi frequencies ($\alpha=1$). Figure 5 shows the absorption spectrum for $\Delta=0$, $\alpha=1$, $\delta=5\Gamma$, and different values of Ω . In this case the spectrum consists of a symmetric series of dispersionlike sidebands located at $\omega_p = \omega_0 \pm n\delta$, where $n=1, 2, \dots$, and, depending on Ω , there can appear a large absorption peak at the central frequency ω_0 . The separations of the sidebands are independent of Ω , but their number increases with Ω . These features can be explained quantitatively in terms of the dressed states of the system and the possible transitions among them. It has been shown [15] that the dressed states group into manifolds in which successive states are separated in energy by

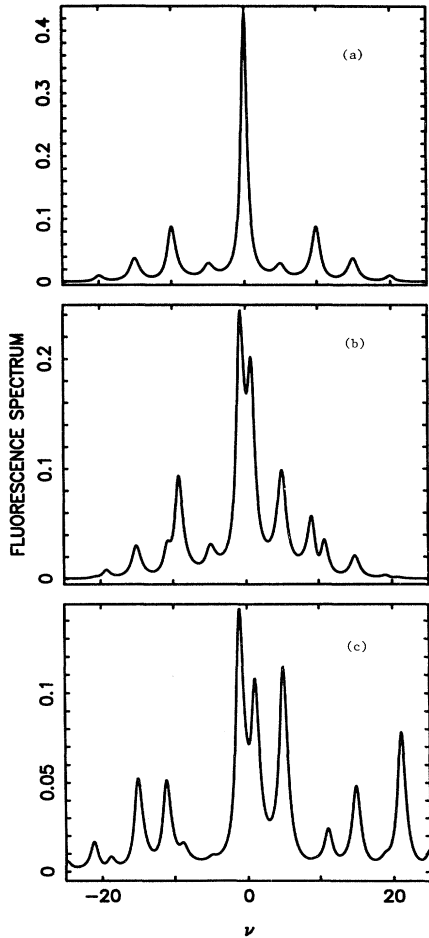


FIG. 4. The fluorescence spectrum as a function of $\nu = (\omega - \omega_s) / \Gamma$ for $\Delta=0$, $\delta=5\Gamma$, $\Omega=8\Gamma$, and different α : (a) $\alpha=1$, (b) $\alpha=0.75$, (c) $\alpha=1.7$.

δ . It is clear that the possible transition frequencies are $\omega_0 \pm n\delta$, where $n=0, 1, 2, \dots$. Due to the symmetric population about $m=0$ of the dressed states, no net absorption or amplification of the probe field is predicted to zero order in $1/\Omega$, as is typical of simple dressed-atom calculations [4]. Thus any absorption or emission features occur in the spectrum as higher-order corrections in $1/\Omega$. It is well known [8–10] that the first-order corrections in $1/\Omega$ produce dispersionlike features, which explains why we observe here a symmetric series of dispersionlike sidebands. However, the model does not explain the presence of the central absorption peak at $\omega_p = \omega_0$, whose amplitude oscillates with the Rabi frequency. This unexpected result can be understood by referring to the Bloch equations (2.4). It is useful to rewrite Eq. (2.4), separating $X_1(t)$ and $X_2(t)$ into two parts. To simplify the notation, we define

$$\begin{aligned} X_1(t) &= U(t) + V(t), \\ X_2(t) &= U(t) - V(t), \\ X_3(t) &= D(t). \end{aligned} \quad (5.8)$$

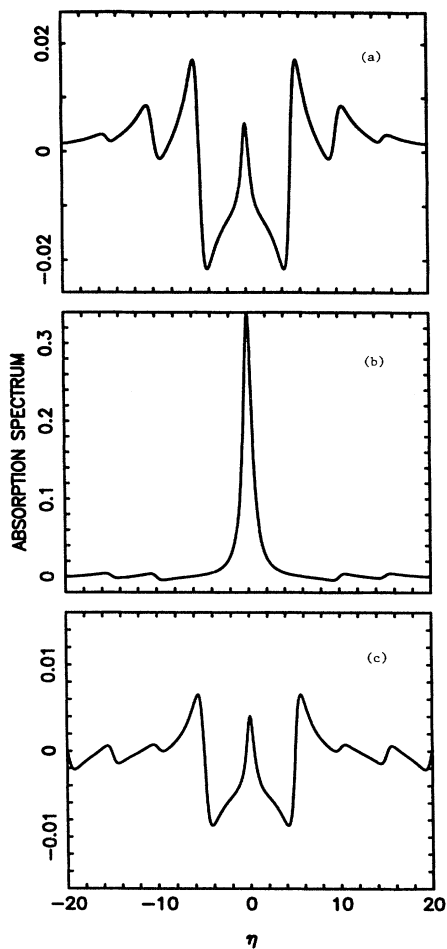


FIG. 5. The absorption spectrum of a weak-probe beam as a function of $\eta = (\omega_p - \omega_s)/\Gamma$ for $\Delta=0$, $\alpha=1$, $\delta=5\Gamma$, and different Rabi frequencies: (a) $\Omega=6\Gamma$, (b) $\Omega=10\Gamma$, (c) $\Omega=14\Gamma$.

For $\Delta=0$ and $\alpha=1$ the homogeneous part of Eq. (2.4) then becomes

$$\begin{aligned} \frac{d}{dt} V(t) &= -\frac{1}{2}\Gamma V(t), \\ \frac{d}{dt} U(t) &= -\frac{1}{2}\Gamma U(t) + \Omega D(t)(e^{-i\delta t} + e^{i\delta t}), \\ \frac{d}{dt} D(t) &= -\Gamma D(t) - \Omega U(t)(e^{-i\delta t} + e^{i\delta t}). \end{aligned} \quad (5.9)$$

It is evident from Eq. (5.9) that the component $V(t)$ is independent of the driving field and is decoupled from the remaining components. Its equation has the simple solution

$$V(t) = V(0)e^{-(1/2)\Gamma t}, \quad (5.10)$$

where $V(0)$ is the initial value of $V(t)$.

Using the quantum regression theorem and the definition (5.7), we write the absorption spectrum as

$$\frac{W(\omega_p)}{W_0} = -\frac{1}{2}\langle S^z \rangle^{(0)} \frac{1}{(\frac{1}{4} + \eta^2)} + 2 \operatorname{Re} U^{(0)}(z)|_{z=-i\eta}, \quad (5.11)$$

where $\langle S^z \rangle^{(0)}$ and $U^{(0)}(z)$ are the zero-order components of the slowly varying amplitudes $\langle S^z \rangle^{(l)}$ and $U^{(l)}(z)$, respectively. It is seen from Eq. (5.11) that the central peak of the absorption spectrum is distinct from the remaining contributions, which depend on the bichromatic driving field. The amplitude of the central peak depends on the zero-order component of the population inversion $\langle S^z \rangle$. Figure 6 illustrates the dependence of the population inversion $\langle S^z \rangle$ on Ω for monochromatic excitation ($\delta=0$), and for bichromatic excitation with $\delta=5\Gamma$. Under monochromatic excitation $\langle S^z \rangle$ steadily increases toward the saturation value $\langle S^z \rangle=0$. When the atom is driven by the bichromatic field we find, in agreement with previ-

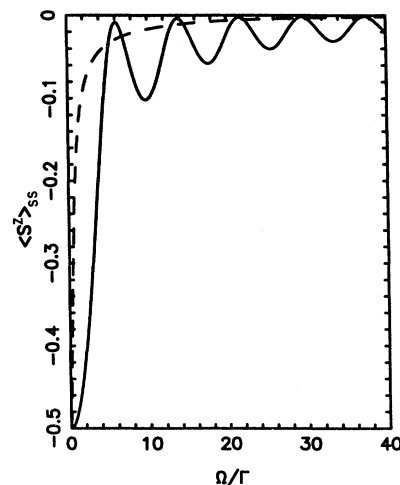


FIG. 6. The steady-state population inversion $\langle S^z \rangle_{ss} = \langle S^z \rangle^{(0)}$ as a function of the Rabi frequency for bichromatic excitation with $\delta=5\Gamma$ (solid line) and for monochromatic excitation (dashed line).

ous results [19–23,27], that the population inversion oscillates as a function of the Rabi frequency. For $\Omega=6\Gamma$, $\langle S^z \rangle \approx 0$ and there is no central peak in the spectrum (see Fig. 5). For $\Omega=10\Gamma$, $\langle S^z \rangle \approx -0.1$ and we observe a pronounced absorption peak at $\eta=0$. A further increase to $\Omega=14\Gamma$ leads to $\langle S^z \rangle \approx 0$ again, accompanied by the disappearance of the central peak.

It should be noted that the central peak of the absorption spectrum can be separated from the remaining contributions only when $\Omega_1=\Omega_2$ and the detuning Δ is zero. For this case, one component of the Bloch vector, $V(t)$, is decoupled from the remaining components, which depend on the driving field. When $\Omega_1 \neq \Omega_2$ and/or $\Delta \neq 0$ all components of the Bloch vector are coupled to the driving field, and the spectrum is more complicated. An illustration of this effect is given in Fig. 7 where we plot the absorption spectrum for $\alpha=1$, $\delta=5\Gamma$, $\Omega=8\Gamma$, and different values of Δ . It is evident from Fig. 7 that the spectrum is altered drastically by changing the detuning Δ . For $\Delta \neq 0$ the central peak and even sidebands split into doublets which contain one absorption and one emission peak, while the odd sidebands are not sensitive to Δ

and remain dispersive. As Δ increases, the splitting increases, as do also the amplitudes of the doublets. Thus for $\Delta \neq 0$ there are regions of frequencies near $\omega_p = \omega_s$ and $\omega_p = \omega_s \pm 2n\delta$, where the probe beam is strongly amplified instead of being absorbed by the atom. In Fig. 8 we plot the spectrum for $\Delta=0$, $\delta=5\Gamma$, $\Omega_1 < \Omega_2$, $\Omega_1 > \Omega_2$, and compare it with that obtained for $\Omega_1 = \Omega_2$. The spectrum is similar to that for $\Delta \neq 0$ and shows absorption and emission peaks near the frequencies $\omega_p = \omega_s \pm 2n\delta$, where $n=0, 1, 2, \dots$. The odd sidebands are not sensitive to Ω_i and remain dispersive independent of the ratio $\alpha = \Omega_2/\Omega_1$. It is interesting to note that for $\Omega_1 > \Omega_2$ the spectrum is similar to that for $\Omega_1 < \Omega_2$, except that the absorption components have become emission components and vice versa. In the next section we give a simple dressed-atom explanation of these features.

VI. THE DRESSED-ATOM MODEL

In Secs. IV and V we calculated and presented graphically the fluorescence and absorption spectra of a two-level atom under a strong bichromatic excitation. We

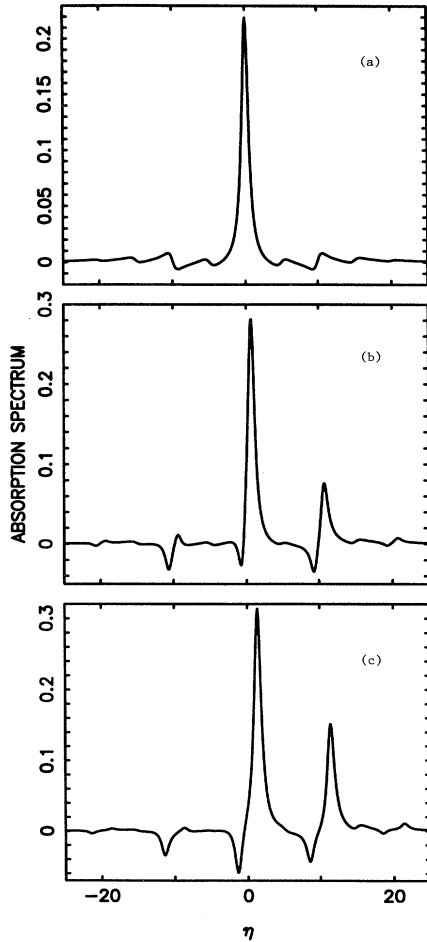


FIG. 7. The absorption spectrum of a weak-probe beam as a function of $\eta = (\omega_p - \omega_s)/\Gamma$ for $\alpha=1$, $\delta=5\Gamma$, $\Omega=8\Gamma$, and detunings (a) $\Delta=0$, (b) $\Delta=2\Gamma$, (c) $\Delta=4\Gamma$.

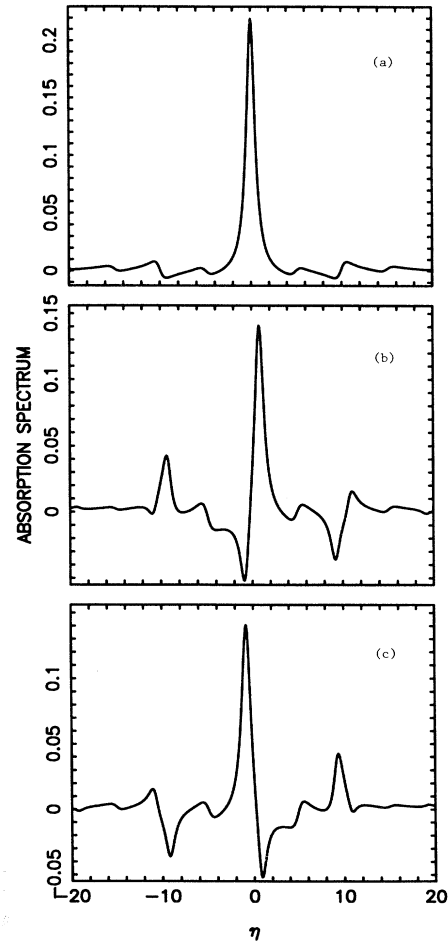


FIG. 8. The absorption spectrum for bichromatic excitation with $\Delta=0$, $\delta=5\Gamma$, and unequal Rabi frequencies: (a) $\Omega_1=\Omega_2=8\Gamma$, (b) $\Omega_1=6\Gamma$ and $\Omega_2=8\Gamma$, (c) $\Omega_1=8\Gamma$ and $\Omega_2=6\Gamma$.

$$\begin{aligned}\lambda^{(1)} &= X^m {}^* P X^m \\ &= \sum_{r,s} X_r^m {}^* P_{rs} X_s^m = \Delta \sum_{\text{even } s} J_{s-m}^2(-\Omega/\delta). \quad (6.12)\end{aligned}$$

Equation (6.12) can be rewritten in two different forms, depending on whether m is even or odd. If m is an even integer, then $s-m$ is even and the summation in Eq. (6.12) yields the result

$$\lambda_e^{(1)} = \frac{1}{2}\Delta[1 + J_0(-2\Omega/\delta)]. \quad (6.13)$$

For m odd, $s-m$ is odd and the summation yields the result

$$\lambda_o^{(1)} = \frac{1}{2}\Delta[1 - J_0(-2\Omega/\delta)]. \quad (6.14)$$

Equations (6.9) and (6.12)–(6.14) are then combined to yield the result

$$\lambda = m\delta + \frac{1}{2}\Delta + (-1)^m u, \quad (6.15)$$

where

$$u = \frac{1}{2}\Delta J_0(-2\Omega/\delta). \quad (6.16)$$

Similarly, to first order the dressed-state energies in manifold $N-1$ turn out to be

$$\lambda = m\delta + \frac{1}{2}\Delta - (-1)^m u. \quad (6.17)$$

The energy levels of the dressed atom are shown in Fig. 9 for $\Delta=0$ and $\Delta>0$. For $\Delta>0$, in the upper manifold the coupling is stronger between the pairs of levels $|en_1 n_2\rangle$ and $|gn_1 n_2 + 1\rangle$ (immediately above) than between $|en_1 n_2\rangle$ and $|gn_1 + 1 n_2\rangle$ (immediately below). Thus there results a net repulsion between the more strongly coupled pairs, as indicated in Fig. 9. For $\Delta=0$, the coupling and repulsion are equal in both directions, resulting in unshifted energies. In the lower manifold, $N-1$, the coupling for $\Delta\neq 0$ produces a reversed pattern

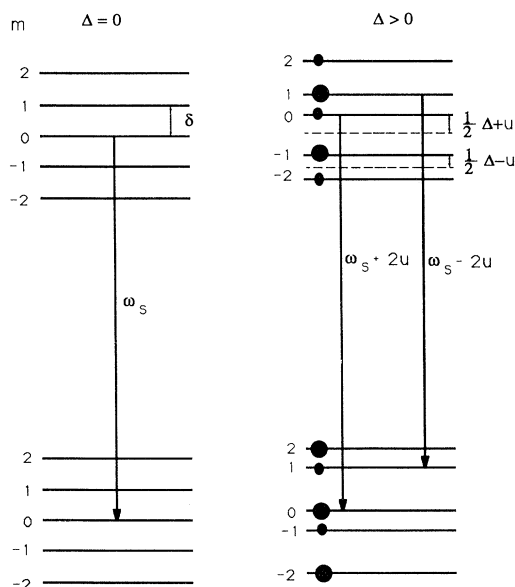


FIG. 9. Eigenstates of the dressed atom for $\Delta=0$ and $\Delta>0$.

of doublet shifts, as illustrated in Fig. 9. It is then easy to see that transitions between the manifolds result in the central peak's and even sidebands' being split into two components (for $\Delta\neq 0$), while the frequencies of the odd sidebands are unaffected.

In order to determine the intensities of the spectral lines and the absorptive and/or dispersive behavior of the components of the absorption spectrum we need the populations of the dressed states. For $\Delta=0$, and to zero order in Γ/Ω , all dressed states in each manifold are equally populated [15,17]. For $\Delta>0$ the odd states ($2m+1$) in the upper manifold are shifted (upwards) from their unperturbed ($\Delta=0$) values by the amount $\frac{1}{2}\Delta - u$, whereas the even states are shifted by $\frac{1}{2}\Delta + u$, as shown in Fig. 9; furthermore, the odd states are more populated than the even (this is indicated in Fig. 9 by the circles). In the absorption spectrum, unequal population of the dressed states leads to a positive or negative absorption. For $\Delta>0$, the absorption spectrum thus consists of emission (amplification) components at $\omega_p = \omega_s \pm 2n\delta - 2u$, where $n=0,1,2,\dots$, and absorption components at $\omega_p = \omega_s \mp 2n\delta + 2u$. The odd sidebands remain dispersionlike, as these result from transitions between states having the same populations to zero order in Γ/Ω .

When the driving fields have unequal Rabi frequencies ($\alpha\neq 1$) and are symmetrically placed about ω_0 ($\Delta=0$) we find the first-order correction to the eigenvalue $\lambda = m\delta$ to be

$$\begin{aligned}\lambda^{(1)} &= X^m {}^* R X^m \\ &= \sum_{r,s} X_r^m {}^* R_{rs} X_s^m \\ &= \Omega(\alpha-1) \sum_n J_{2n-m} \left[\frac{-\Omega}{\delta} \right] J_{2n-1-m} \left[\frac{-\Omega}{\delta} \right]. \quad (6.18)\end{aligned}$$

Equation (6.18) can be rewritten in two different forms. If m is an even (odd) integer, then $2n-m$ is even (odd), and $2n-m-1$ odd (even). In both cases, using the symmetry properties of the Bessel functions and Eq. (21) of Ref. [15], we obtain

$$\lambda = m\delta + (-1)^m w, \quad (6.19)$$

where

$$w = \frac{1}{2}\Omega(\alpha-1)J_1(2\Omega/\delta). \quad (6.20)$$

Similarly, to first order the dressed-state energies in manifold $N-1$ turn out to be

$$\lambda = m\delta + (-1)^{m+1} w. \quad (6.21)$$

The energy levels of the dressed atom are shown in Fig. 10 for $\alpha=1$, $\alpha<1$, and $\alpha>1$. For $\alpha<1$, $\Omega_1>\Omega_2$; in the upper manifold, the coupling is stronger between the pairs of levels $|en_1 n_2\rangle$ and $|gn_1 + 1 n_2\rangle$ (immediately below) than between $|en_1 n_2\rangle$ and $|gn_1 n_2 + 1\rangle$ (immediately above). Thus there results a net repulsion between the more strongly coupled pairs, as indicated in Fig. 10. For $\Omega_2>\Omega_1$, the coupling is stronger between the pairs $|en_1 n_2\rangle$ and the levels immediately above, $|gn_1 n_2 + 1\rangle$;

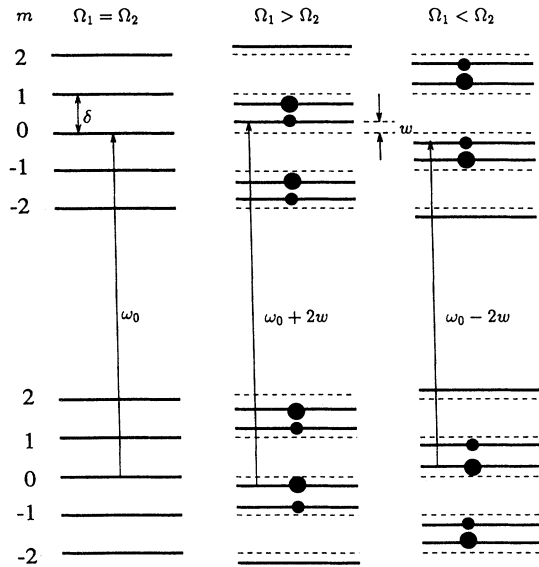


FIG. 10. Eigenstates of the dressed atom for $\Omega_1 = \Omega_2$, $\Omega_1 > \Omega_2$, and $\Omega_1 < \Omega_2$.

the resulting net repulsion is pictured in Fig. 10. For $\alpha = 1$, the coupling and repulsion is equal in both directions, resulting in unshifted energies. In the lower manifold, the coupling for $\alpha < 1$ and $\alpha > 1$ produces a reversed pattern of doublet shifts. As a result transitions between the manifolds lead to the central peak's and even sidebands' being split into two components (for $\alpha \neq 1$), while the frequencies of the odd sidebands are unaffected.

The population of the dressed states can be found similarly as for the case $\Delta \neq 0$. For $\alpha = 1$ the dressed states are equally populated, while for $\alpha \neq 1$ the shifts of the dressed states lead to unequal population. It is well known from the dressed-atom theory [12] that for driving fields tuned below ω_0 there is more population in the lower dressed state of each doublet than in the upper one (indicated in Fig. 10 by the circles). Consequently, the spectrum for $\alpha < 1$ consists of emission components at $\omega_p = \omega_0 \pm 2n\delta - 2w$, where $n = 0, 1, 2, \dots$, and absorption components at $\omega_p = \omega_0 \mp 2n\delta + 2w$. The odd sidebands remain dispersionlike, as these result from transitions between states having the same populations to zero order in (Γ/Ω) . For $\alpha > 1$ ($\Omega_2 > \Omega_1$) the reverse pattern occurs: The spectrum consists of absorption components at $\omega_p = \omega_0 \pm 2n\delta - 2w$, emission components at $\omega_p = \omega_0 \mp 2n\delta + 2w$, and dispersive features at $\omega_p = \omega_0 \pm (2n + 1)\delta$.

Numerical calculations of the absorption spectrum presented here for $\Omega_1 \neq \Omega_2$ and based on the Bloch equations agree with the physical dressed-atom predictions. Similar agreement between these two models is found in the calculations of the absorption spectrum under off-resonance excitation ($\Delta \neq 0$). When $\Delta = 0$ and $\Omega_1 = \Omega_2$ one component of the Bloch vector is decoupled from the field, and there is disagreement between the two models. When all components of the Bloch vector are coupled to the driving field the dressed-atom model provides a useful physical picture, but is quantitatively correct only for

very high field intensities, whereas the predictions of the optical Bloch equations are correct for all intensities.

VII. SUMMARY

In this paper we have determined the spectral behavior of the fluorescent field radiated by a two-level atom driven by a strong bichromatic field. We have presented a solution for this system obtained by a numerical inversion of an infinite matrix. The effects of detuning and of unequal Rabi frequencies on the steady-state intensity, fluorescence, and absorption spectra has been discussed in detail. For a weak driving field with equal intensities the power broadening spectrum shows two peaks located at $\Delta = \pm\delta$. As the intensity of the driving field increases, these peaks move towards smaller Δ and simultaneously become power broadened. In addition, there appear new peaks at frequencies $\Delta \approx \pm 3\delta$. For a strong driving field, the spectrum exhibits resonances at $\Delta = \pm n\delta \mp \Omega^2/4\delta$, where n is an odd integer. This result predicts the intensity-dependent shift, $(\Omega^2/4\delta)$, which is the generalized Bloch-Siegert shift extensively discussed for a two-level atom in a fully modulated field [21,33–36]. The fluorescence spectrum for the atom in an off-resonance bichromatic field shows more peaks than for resonant excitation. This interesting phenomenon is due to the splitting of the central peak and the even sidebands into doublets, whose positions and intensities depend on both Δ and Ω . The same behavior is found for a resonant bichromatic field with unequal Rabi frequencies.

The absorption spectrum of a weak-probe beam for $\Delta = 0$ and $\Omega_1 = \Omega_2$ shows a symmetric series of dispersionlike sidebands separated by the constant spacing δ , and an absorption peak at the central frequency $\omega_p = \omega_0$ whose amplitude oscillates with Ω . These features of the absorption spectrum *cannot* be explained by the simple dressed-atom model. Dressed-atom calculations (to zero order in Γ/Ω) predict equal population of the dressed states, and therefore no absorption, amplification, or dispersion of the probe field. The spectral features for $\Delta = 0$ and $\Omega_1 = \Omega_2$ require calculations which include terms inversely proportional to the Rabi frequency. In the off-resonance case $\Delta \neq 0$ and/or $\Omega_1 \neq \Omega_2$ a new feature develops: the central peak and the even sidebands split into absorption-emission doublets, whereas the odd sidebands remain dispersionlike. In this case there are more regions of frequency where the probe beam is amplified instead of being absorbed by the atom. The spectral features for $\Delta \neq 0$ and/or $\Omega_1 \neq \Omega_2$ are qualitatively explained by the dressed-atom model. The splitting of the spectral lines is directly related to the shifted dressed-atom frequencies, and the absorption-emission behavior of the absorption spectrum is related to the unequal population of the dressed states.

ACKNOWLEDGMENTS

One of the authors (Z.F.) gratefully acknowledges discussions with J. D. Cresser, P. D. Drummond, and B. J. Dalton. This work was supported in part by the Australian Research Council and the Natural Sciences and Engineering Research Council of Canada, to whom the authors extend their thanks.

- [1] B. R. Mollow, *Phys. Rev.* **188**, 1969 (1969).
- [2] H. J. Carmichael and D. F. Walls, *J. Phys. B* **9**, 1199 (1976).
- [3] H. J. Kimble and L. Mandel, *Phys. Rev. A* **13**, 2123 (1976).
- [4] C. Cohen-Tannoudji and S. Reynaud, *J. Phys. B* **10**, 345 (1977).
- [5] F. Y. Wu, R. E. Grove, and S. Ezekiel, *Phys. Rev. Lett.* **35**, 1426 (1975).
- [6] N. Lu, P. R. Berman, Y. S. Bai, J. E. Golub, and T. W. Mossberg, *Phys. Rev. A* **34**, 319 (1986).
- [7] H. J. Kimble and L. Mandel, *Phys. Rev. A* **15**, 689 (1977); P. L. Knight, W. A. Molander, and C. R. Stroud, Jr., *ibid.* **17**, 1547 (1978).
- [8] B. R. Mollow, *Phys. Rev. A* **5**, 2217 (1972).
- [9] G. S. Agarwal, *Phys. Rev. A* **19**, 923 (1979); G. Grynberg and C. Cohen-Tannoudji, *Opt. Commun.* **96**, 150 (1993).
- [10] S. Yeh, *J. Phys. B* **15**, 3223 (1982); Z. Ficek, R. Tanaś, and S. Kielich, *ibid.* **17**, 1491 (1984); B. J. Dalton and M. Gagen, *ibid.* **18**, 4403 (1985); H. S. Freedhoff, *ibid.* **11**, 811 (1978); N. Lu and P. R. Berman, *Phys. Rev. A* **36**, 3845 (1987).
- [11] F. Y. Wu, S. Ezekiel, M. Ducloy, and B. R. Mollow, *Phys. Rev. Lett.* **38**, 1077 (1977).
- [12] C. Cohen-Tannoudji, J. Dupont-Roc, and G. Grynberg, *Atom-Photon Interactions* (Wiley, New York, 1992).
- [13] Y. Zhu, A. Lezama, Q. Wu, and T. W. Mossberg, in *Coherent and Quantum Optics VI*, edited by J. H. Eberly, L. Mandel, and E. Wolf (Plenum, New York, 1989), p. 1297; Y. Zhu, Q. Wu, A. Lezama, D. J. Gauthier, and T. W. Mossberg, *Phys. Rev. A* **41**, 6574 (1990).
- [14] G. Yu. Kryuchkov, *Opt. Commun.* **54**, 19 (1985).
- [15] H. S. Freedhoff and Z. Chen, *Phys. Rev. A* **41**, 6013 (1990); **46**, 7328(E) (1992).
- [16] S. P. Tewari and M. K. Kumari, *Phys. Rev. A* **41**, 5273 (1990).
- [17] G. S. Agarwal, Y. Zhu, D. J. Gauthier, and T. W. Mossberg, *J. Opt. Soc. Am. B* **8**, 1163 (1991).
- [18] S. Feneuille, M. G. Schweighofer, and G. Oliver, *J. Phys. B* **9**, 2003 (1976).
- [19] P. Thomann, *J. Phys. B* **13**, 1111 (1980).
- [20] B. Blind, P. R. Fontana, and P. Thomann, *J. Phys. B* **13**, 2717 (1980).
- [21] W. M. Ruyten, *J. Opt. Soc. Am. B* **6**, 1796 (1989); **9**, 1892 (1992).
- [22] H. Friedmann and A. D. Wilson-Gordon, *Phys. Rev. A* **36**, 1336 (1987).
- [23] G. S. Agarwal and N. Nayak, *J. Phys. B* **19**, 3385 (1986).
- [24] M. Wilkens and K. Rzążewski, *Phys. Rev. A* **40**, 3164 (1989).
- [25] M. A. Newbold and G. J. Salamo, *Phys. Rev. A* **22**, 2098 (1980).
- [26] G. S. Agarwal and Y. Zhu, *Phys. Rev. A* **46**, 479 (1992).
- [27] S. Chakmakijan, K. Koch, and C. R. Stroud, Jr., *J. Opt. Soc. Am. B* **5**, 2015 (1988).
- [28] H. Ritsch, P. Zoller, and J. Cooper, *Phys. Rev. A* **41**, 2653 (1990).
- [29] R. M. Whitley and C. R. Stroud, Jr., *Phys. Rev. A* **14**, 1498 (1976).
- [30] G. S. Agarwal, in *Quantum Optics*, edited by G. Hohler, Springer Tracts in Modern Physics Vol. 70 (Springer, Berlin, 1974).
- [31] F. Bloch and A. Siegert, *Phys. Rev.* **57**, 522 (1940).
- [32] L. Allen and J. H. Eberly, *Optical Resonance and Two-Level Atoms* (Wiley, New York, 1975), p. 47.
- [33] F. Ahmad and R. K. Bullough, *J. Phys. B* **7**, L275 (1974).
- [34] S. Stenholm, *J. Phys. B* **5**, 878 (1972).
- [35] P. Hannaford, D. T. Pegg, and G. W. Series, *J. Phys. B* **6**, L222 (1973).
- [36] S. Swain, *J. Phys. B* **7**, 2363 (1974).
- [37] M. Lax, *Phys. Rev.* **172**, 350 (1968).
- [38] B. J. Dalton, in *Coherence and Quantum Optics V*, edited by L. Mandel and E. Wolf (Plenum, New York, 1984), p. 791.
- [39] N. Nayak and G. S. Agarwal, *Phys. Rev. A* **31**, 3175 (1985).
- [40] A. M. Bonch-Bruевич, T. A. Vartanyan, and N. A. Chigier, *Zh. Eksp. Teor. Fiz.* **77**, 1899 (1979) [*Sov. Phys. JETP* **50**, 901 (1979)].